HHS Public Access

Author manuscript

Org Biomol Chem. Author manuscript; available in PMC 2019 November 28.

Published in final edited form as:

Org Biomol Chem. 2018 November 28; 16(46): 8976–8983. doi:10.1039/c8ob02596g.

New Tetralactam Hosts for Squaraine Dyes†

Janel M. Dempsey[#], **Qi-Wei Zhang**[#], **Allen G. Oliver**, and **Bradley D. Smith**[*]

Department of Chemistry and Biochemistry, 236 Nieuwland Science Hall, University of Notre Dame, Notre Dame, IN 46556, USA.

[#] These authors contributed equally to this work.

Abstract

The photophysical properties of a deep-red fluorescent squaraine dye can be improved by encapsulating it within a tetralactam macrocycle. Three new tetralactams are described with different substituents (methyl, methoxy, methylenedioxy) on the macrocycle aromatic sidewalls. The capability of each tetralactam to encapsulate a squaraine dye in chloroform solution was determined experimentally using absorption, fluorescence, and NMR spectroscopy. Two of the tetralactams were found to thread a squaraine dye with association constants on the order of 10^6 M^{-1}, while a third macrocycle exhibited no squaraine affinity. An X-ray crystal structure of the third tetralactam showed that the substituents sterically blocked squaraine association. Of the two tetralactams that encapsulate a squaraine, one induces an increase in squaraine fluorescence quantum yield, while the other quenches the squaraine fluorescence. The results suggest that these new squaraine binding systems will be useful for biological imaging and diagnostics applications.

Graphical Abstract

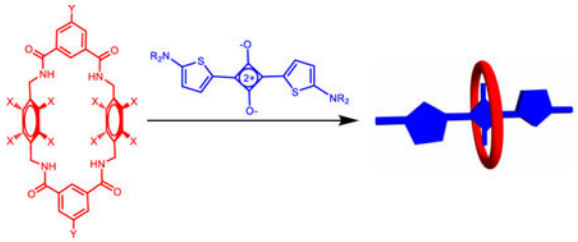

Tetralactam macrocycles with similar substituents (methyl, methoxy, methylenedioxy) on the macrocycle aromatic sidewalls have very different squaraine recognition properties.

Introduction

The supramolecular chemistry of tetralactam macrocycles has been an active research topic for several decades, and researchers have demonstrated host association with a wide range of

†Electronic Supplementary Information (ESI) available: [NMR and absorption/emission spectra, titration data]. See DOI: 10.1039/x0xx00000x

* smith.115@nd.edu.

Conflicts of interest

There are no conflicts to declare.

neutral and charged guests.[1–8] Our group has focused on tetralactam hosts that encapsulate deep-red fluorescent squaraine dyes. Our early work developed Leigh-type "clipping reactions" that assembled the macrocycle around a dumbbell-shaped dye to create a permanently interlocked squaraine rotaxane.[9] We have also prepared squaraine rotaxanes by conducting "capping reactions" that threaded a macrocycle with a suitable dye precursor and then covalently attached stopper groups to each end of the encapsulated dye.[10] More recently, we expanded the structural scope of the macrocycle threading process by quantifying the thermodynamic and kinetics for a wide range of different squaraine derivatives.[11–12] We have demonstrated that macrocycle/squaraine complexes can be pre-assembled with sufficiently high stability for deployment as fluorescent probes for biological imaging.[13] In other cases, we have shown that the change in fluorescence properties produced by the squaraine threading process can be exploited as a signaling mechanism for diagnostic applications.[14]

To date, most of our macrocycle threading work in organic solvents has involved tetralactam **M1** (Scheme 1), which is a highly preorganized macrocycle with four convergent amide NH bonds and two parallel anthracene sidewalls. Encapsulation of a squaraine dye such as **S1** is highly favored by the simultaneous formation of strong hydrogen bonds between the macrocycle NH resides and the squaraine oxygens and stacking interactions between the dye and macrocycle aromatic surfaces. Upon encapsulation, the absorption and emission maxima bands of the squaraine are red-shifted by 20–30 nm, a phenomenon that has been attributed to attenuated deformation of the amine substituents at each end of the squaraine structure.[15] While **M1** and its derivatives remain a valuable macrocycle family for further development as supramolecular hosts, there are some drawbacks in certain applications. For example, the anthracene sidewalls are susceptible to photooxidation, and several derivatives have been found to have relatively poor solubility. Thus, there is a need for analogous tetralactams with structurally different sidewalls. A few years ago we investigated the squaraine threading ability of the well-known tetralactam **M2** which has two angular and electron-rich diphenylmethane sidewalls.[1–2, 10] Compared to **M1**, the squaraine affinity in organic solvent was 40-fold lower, and there was a significance decrease in squaraine fluorescence quantum yield.[10] A major reason for the decreased squaraine affinity is the reduced amount of aromatic stacking due to the angular sidewalls of **M2**. Therefore, we decided to design a new set of preorganized tetralactam macrocycles with parallel sidewalls.

In this current report, we describe the squaraine encapsulation properties of tetralactams **M3**, **M4**, and **M5** in organic solvent. Recently, we prepared **M3** and found that it can encapsulate several different anionic square planar metal complexes.[16] An X-ray crystal structure of the empty macrocycle showed that it adopts a highly preorganized structure with four convergent amide NH bonds and two parallel 2,3,5,6-tetramethylbenzene sidewalls; thus, we expected the internal cavity to be highly complementary for squaraine guests. Tetralactams **M4** and **M5** are new structures that have four oxygen substituents on each aromatic sidewall. We expected the oxygen substituents to increase the π-electron density on the sidewalls and perhaps enhance electrostatic stacking interactions with the electron-deficient C_4O_2 core of an encapsulated squaraine dye. In the case of **M4**, it was not clear how the four methoxy groups on each sidewall would sterically arrange themselves and if they would block access

of a squaraine guest to the macrocycle cavity. In the case of **M5**, these putative steric effects are removed by incorporating the oxygens atoms into benzodioxo rings which produces sidewalls that are essentially flat and parallel. In the following sections, we describe the synthesis and structure of the new tetralactams. In addition, we have conducted a series of spectroscopic studies that mixed each macrocycle with squaraine **S1** in chloroform solvent and determined if a macrocycle/squaraine complex was formed. When a complex was formed we measured the association constant by conducting titration experiments and quantified the photophysical properties of the encapsulated squaraine.

Results and discussion

Synthesis

The syntheses of macrocycles **M1**, **M2**, and **M3** and squaraine **S1** have been previously reported.[12, 16–17] Shown in Scheme 2 is the preparation of new tetralactams **M4a**, **M4b**, and **M5**. Starting material **1** was obtained in nearly quantitative yield following tin-mediated reduction of commercially available 2,5-dihydroxy-1,4-benzoquinone.[19] Alkylation of **1** with dimethyl sulfate produced **2**, which was reacted with bromomethyl methyl ether to yield **3**.[20–21] Bis(bromomethyl) **3** was converted to bis-amine **4**[17], which was reacted separately with acid chlorides **5** or **6** under diluted conditions to yield macrocycles **M4a** and **M4b**, respectively. The starting material **7** was prepared by reacting **1** with dibromomethane under basic conditions. The same sequence as above was followed to give macrocycle **M5**.

Squaraine Threading of M3

Shown in Figure 1 are the important ^{1}H NMR spectral changes that occurred when macrocycle **M3** and squaraine **S1** were mixed at a 1:1 molar ratio in $CDCl_3$. The spectra show several large changes in chemical shift that are diagnostic of macrocycle threading by the dye to produce **M3⊃S1**. Most notably, the signals for squaraine protons 1 and 2 sharpen and are shifted upfield, indicating increased dye rigidity and magnetic shielding by the surrounding aromatic sidewalls of **M3**. The signals for the macrocycle NH and protons B are strongly shifted downfield indicating hydrogen bonding with the oxygen atoms of the encapsulated squaraine guest. Furthermore, there are two signals for macrocycle protons B in a ratio of about 1:1, a phenomenon that also occurs when **S1** is encapsulated by **M1**.[11–12] The two different signals (one is a single peak and the other is a pair of single peaks) correspond to the two conformational isomers that can be adopted by encapsulated **S1**. The relative orientation of the two thiophene units in **S1** can be either cis or trans, and when the conformation of the encapsulated squaraine is cis the two macrocycle protons B are chemically inequivalent. The amide protons of **M3** are also split into a single peak and two sets of single peaks and protons C are split into two sets of signals due to the two conformations of encapsulated **S1** (Figure S15).

Threading of **M3** by **S1** was confirmed by absorption and fluorescence spectroscopy. Addition of one molar equivalent of **M3** to a 3.0 μM solution of **S1** in $CHCl_3$ produced an 8 nm red shift in the squaraine absorption band and a 19 nm red shift in the squaraine emission band. These red shift effects are indicative of squaraine encapsulation, although the changes are smaller than those observed when **S1** is encapsulated by **M1**.[11–12] As stated above, the

red shift effect is due to attenuated deformation of the amine substituents at each end of the squaraine structure.[15] Thus, the relative difference is attributed to the narrower width of the cavity sidewalls in **M3**, which means the amine groups at each end of the encapsulated squaraine structure are not as constrained.[15] The spectra in Figure 2 show that encapsulation of **S1** inside **M3** produces a slight decrease in molar absorptivity but a substantial increase in fluorescence intensity. Indeed, the fluorescence quantum yield for free **S1** in $CHCl_3$ is increased five-fold when it is converted into **M3⊃S1** (Table 1).

The large enhancements in fluorescence emission induced by squaraine encapsulation made it straightforward to conduct fluorescence titration experiments which provided the association data in Table 2. Shown in Figure S16 is a titration isotherm that was produced by adding aliquots of **M3** to **S1** in $CHCl_3$. Using a standard non-linear computer algorithm, the curve was fitted to a 1:1 binding model and a value of $K_a = 5.1 \times 10^6\ M^{-1}$ was determined, which is an order of magnitude lower than the K_a determined previously for threading of **M1** by **S1**.[12] This decrease in affinity is attributed to the lower aromatic surface area of the macrocycle sidewalls which weakens stacking interactions with the encapsulated dye. The rate constant for threading of **M3** by **S1** was measured by monitoring the fluorescence increase due to appearance of the complex over time. The kinetic profile (Figure S17) was fitted to second-order kinetic model to give a rate constant (k_{on}) of $9.1 \times 10^3\ M^{-1}\ s^{-1}$, which is an order of magnitude slower than the threading of **M1** by **S1**.[12] This decrease in k_{on} is attributed to steric hindrance by the sidewall methyl groups on **M3** that inhibit entry of **S1** into the macrocyclic cavity.

No Squaraine Threading of M4a

Macrocycle **M4a** is an analogue of **M3** with methoxy groups instead of methyl groups on the two macrocyclic sidewalls. A collection of different spectroscopic experiments all suggested that **S1** was unable to thread **M4a** in chloroform, even after standing for 24 hours. The ^1H NMR spectra in Figure S18 show no change in chemical shift for either the macrocycle or dye protons when the compounds were mixed in $CDCl_3$. The absorption and fluorescence spectra in Figure 3 show that addition of **M4a** to **S1** produced no change in squaraine absorption maxima wavelength and no change in squaraine emission spectra. A lack of interaction was also observed when **M4a** or the closely related macrocycle **M4b** were mixed in solution with two other structurally related squaraine dyes (Figures S19 and S20).

An explanation for the lack of squaraine encapsulation was gained by analyzing an X-ray crystal structure of **M4b**. The molecular pictures in Figure 4 highlight some important structural features that are induced by the four methoxy groups on each macrocycle sidewall. To relieve steric congestion, each pair of adjacent methoxy groups adopts a trans orientation relative to the plane of a phenyl sidewall (Figure 4d). Thus, with each macrocycle sidewall two methoxy groups are directed towards the macrocyclic cavity and two point away. The inward facing methoxy groups inhibit macrocycle threading in two ways: (a) they sterically block front and rear access of a squaraine guest to the macrocycle cavity (Figure 4b), (b) they force two of the four macrocycle amide NH residues to be directed out of the

macrocyclic cavity creating a C_2-symmetric host conformation that does not have a complementary shape for a squaraine guest (Figure 4c).[22]

Squaraine Threading of M5

To obviate the steric congestion created by the methoxy groups in **M4** we designed macrocycle **M5**, which incorporates the adjacent sidewall oxygens into benzodioxole rings and creates macrocycle sidewalls that are essentially planar and parallel. The limited solubility of macrocycle **M5** in chloroform required the use of a $CDCl_3/CD_3OD$ solvent system for NMR studies. Figure 5 shows the important ^1H NMR spectral changes that occurred when macrocycle **M5** and squaraine **S1** were mixed at a 1:1.1 molar ratio. As in the case of **M3⊃S1** in Figure 1 above, there are several large changes in chemical shift indicating the formation of **M5⊃S1**. The signals for squaraine protons 1 and 2 are shifted upfield, and the macrocycle protons B are shifted far downfield. Moreover, there are two signals for protons B (a single peak and a pair of single peaks) corresponding to the cis and trans conformations that can be adopted by the encapsulated **S1**. It is worth noting that there are no NH signals in the ^1H NMR spectrum of free **M5** due to proton-deuterium exchange with the CD_3OD, but NH signals are present in the spectrum of **M5⊃S1**. The difference in proton-deuterium exchange is because the amide protons in free **M5** are much more exposed to the solvent than the amide protons in **M5⊃S1**. The same phenomenon is also observed with permanently interlocked squaraine rotaxanes.[22] As with **M3⊃S1**, there are multiple peaks for the amide protons and protons C of **M5**, corresponding to the two conformations of encapsulated **S1** (Figure S21).

The threading of **M3** was also studied by absorption and fluorescence methods. Interestingly, free **M5** exhibits a moderate absorption band at 325 nm, with broad emission at 480 nm (Figure S14). While this optical property was not directly relevant to the present study which focused on the changes in squaraine fluorescence induced by the macrocycle, it does raise the possibility that suitable derivatives of **M5** may have future value as a fluorescent host for non-fluorescent guests such as biomedically important saccharides.[23–24]

As expected, **S1** was able to thread **M5**, a process that produced a 7 nm red shift in squaraine absorption (Figure 6a). Interestingly, a blue-shifted shoulder appeared in the squaraine absorption spectrum indicating self-aggregation of the threaded complex, **M5⊃S1**, a phenomenon that is in line with the relatively low solubility of the complex (Figure S22). Fluorescence spectra of the samples showed that the emission of **S1** is strongly quenched when it is encapsulated inside **M5** (Figure 6b). This is in contrast to the fluorescence enhancement that is observed when **S1** is encapsulated by **M1** or **M3**. There are two contributing factors for the squaraine quenching by **M5**. One factor is the highly electron-rich aromatic sidewalls in **M5** which can deactivate the excited state of encapsulated **S1** by photoinduced electron transfer. This explanation is supported by the literature knowledge that squaraines are quenched when covalently linked to electron-rich aromatic rings,[25] and also when they are encapsulated by macrocycle **M2** which also has electron-rich sidewalls.[10] The other reason for the diminished fluorescence of **M5⊃S1** is the self-aggregation which is known to promote excited state quenching due to energy transfer between multiple chromophores within an aggregate.[26] A fluorescence titration experiment that added aliquots

of **M5** to **S1** in $CHCl_3$ produced a curve (Figure S23) that was fitted to a 1:1 binding model, and produced an association constant of $8.6 \times 10^5\ M^{-1}$, approximately six times lower than the **S1** affinity displayed by **M3**. Thus, we did not confirm our hypothesis that tetralactam affinity for squaraine dyes would be improved by using macrocycles with increased π-electron density on the macrocycle sidewalls. On the other hand, new tetralactam **M5** has higher squaraine affinity than **M2**, which is the only other tetralactam known to quench the fluorescence of an encapsulated squaraine. As we have shown previously with **M2**, it should be possible to develop molecular shuttles or binding assays that "turn on" fluorescence when a squaraine is displaced from the quenching confines of **M5**.[10, 27]

Conclusion

Macrocycles **M3** and **M5** are two new tetralactams with highly preorganized structures and open cavities that can encapsulate squaraine dyes with high affinity in chloroform solution. Squaraine threading of **M3** leads to enhancement of squaraine fluorescence, whereas threading of **M5** leads to quenching of squaraine fluorescence. A third macrocycle, **M4**, has no squaraine affinity due to the steric effects imposed by the methoxy groups on the macrocyclic sidewalls. The next step in the project is to determine if water-soluble versions of **M3** can be threaded by squaraine dyes to create pre-assembled fluorescent probes for biological imaging. It should also be possible to exploit the squaraine quenching ability of macrocycle **M5** and create threaded molecular shuttles or squaraine displacement systems that indicate the presence of analytes with large changes in deep-red fluorescence intensity.

Experimental

Materials

^1H and ^{13}C NMR spectra were recorded on Bruker AVANCE III HD 400 and 500 MHz spectrometers. Chemical shift is presented in ppm and referenced by residual solvent peak. Mass spectrometry (MS) was performed using a Bruker microTOF II spectrometer. Reactions were monitored by TLC plate (precoated with 60 Å silica gel, F254) purchased from SILICYCLE and visualized by UV light (254, 365 nm). Flash column chromatography was performed using silica gel (silicaFlash P60 from SILICYCLE) as the stationary phase. Absorption spectra were collected using an Evolution 201 UV-Vis Spectrometer with ThermoInsight software. Fluorescence spectra were collected using a Horiba Fluoromax-4 Fluorometer with FluorEssence software. Tetralactam macrocycles **M1**,[17] **M2**,[18] and **M3**;[16] squaraine **S1**;[12] acid chlorides **5**[28] and **6**;[29] and hydroquinone derivatives **1**,[19] **2**,[20] and **3**[21] were synthesized according to previously reported procedures.

Synthesis of Bisamine 4

1,4-Bis(bromomethyl)-2,3,5,6-tetramethoxybenzene **3** (2.0 g, 5.24 mmol) and hexamethylenetetramine (2.2 g, 15.71 mmol) were dissolved in chloroform (120 mL) and refluxed for 24 hours. The white precipitate was collected by filtration and washed with cold chloroform. The solid was then dispersed into a solution of ethanol (100 mL) and concentrated hydrochloric acid (20 mL) and refluxed for 24 hours. The flask was then cooled to 0° C and the solid was collected by filtration, washed with cold ethanol, and

allowed to dry in open air. The solid was then stirred in 10% sodium carbonate solution (200 mL), chloroform (80 mL) was added while stirring, and the biphasic solution was separated. The aqueous layer was further extracted with chloroform (3 × 50 mL) and the combined organic phases were dried over anhydrous sodium sulfate. The solvent was removed and the product dried in vacuo to give **4** as a white solid (1.06 g, 79%). ^{1}H NMR (400 MHz, CD_3CN, 25 °C): δ 3.83 (s, 12H), 3.75 (s, 4H). ^{13}C NMR (100 MHz, CD_3CN, 25 °C): δ 148.68, 131.59, 61.82, 36.81. HRMS (ESI-TOF) m/z: $[M+H]^+$ Calcd for $C_{12}H_{21}N_2O_4^+$ 257.1496; Found 257.1506.

Synthesis of Macrocycle M4a

A solution of acid chloride **5** (100 mg, 0.39 mmol) in dry chloroform (100 mL) was added by syringe pump to a solution of bisamine **4** (100 mg, 0.39 mmol) and triethylamine (500 μL) in dry chloroform (200 mL) over 24 hours. After complete addition, the mixture was stirred for an additional 24 hours. The solvent was then removed and the residue purified by column chromatography (1:3 $CHCl_3$:ethyl acetate) to give **M4a** as a white solid (35 mg, 10%). ^{1}H NMR (500 MHz, $CDCl_3$, 25 °C): δ 7.92 (s, 4H), 7.82 (s, 2H), 6.80 (t, J = 5.9 Hz, 4H), 4.70 (d, J = 5.8 Hz, 8H), 3.88 (s, 24H), 1.32 (s, 18H). ^{13}C NMR (100 MHz, $CDCl_3$, 25 °C): δ 166.46, 152.64, 147.94, 134.93, 127.41, 125.63, 122.24, 61.17, 35.23, 34.22, 31.37. HRMS (ESI-TOF) m/z: $[M+H]^+$ Calcd for $C_{48}H_{61}N_4O_{12}^+$ 885.4280; Found 885.4303.

Synthesis of Macrocycle M4b

A solution of acid chloride **6** (500 mg, 1.95 mmol) in dry chloroform (50 mL) was added by syringe pump to a solution of bis-amine **4** (500 mg, 1.95 mmol) and triethylamine (2.7 mL) in dry chloroform (500 mL) over 24 hours. When the addition was completed, the mixture was stirred for an additional 24 hours. The solvent was removed and the residue was purified by column chromatography (1:3 $CHCl_3$:ethyl acetate) to give **M4b** as a white solid (361 mg, 42%). ^{1}H NMR (400 MHz, $CDCl_3$, 25 °C): δ 7.50 (s, 4H), 7.45 (s, 2H), 6.71 (s, 4H), 4.77 (s, 4H), 4.65 (d, J = 5.9 Hz, 8H), 3.83 (s, 24H), 2.55 (s, 2H). ^{13}C NMR (100 MHz, $CDCl_3$, 25 °C): δ 166.03, 158.01, 147.70, 137.10, 125.94, 118.33, 116.53, 77.81, 76.50, 60.97, 56.46, 34.03. HRMS (ESI-TOF) m/z: $[M+H]^+$ Calcd for $C_{46}H_{49}N_4O_{14}^+$ 881.3240; Found 881.3234.

Synthesis of Benzodioxole 7

1,2,4,5-Tetrahydroxybenzene **1** (17 g, 120 mmol), dibromomethane (41 g, 239 mmol) and K_2CO_3 (166 g, 1200 mmol) were stirred in DMF (200 mL) at 90 °C for 24 hours. After cooling to room temperature, the solid was removed by filtration. The filtrate was concentrated and the residue purified by column chromatography (5:1 hexane:CH_2Cl_2) to give **7** as a white solid (2.98 g, 15%). ^{1}H NMR (400 MHz, $CDCl_3$, 25 °C): δ 6.49 (s, 2H), 5.87 (s, 4H). ^{13}C NMR (100 MHz, $CDCl_3$, 25 °C): δ 141.47, 101.41, 93.38. HRMS (ESI-TOF) m/z: $[M+H]^+$ Calcd for $C_8H_7O_4^+$ 167.0339; Found 167.0311.

Synthesis of Bisbromo 8

To a stirred solution of compound **7** (2.0 g, 12.04 mmol) in 20 mL trifluoroacetic acid was added bromomethyl methyl ether (3.73 g, 1.8 mL, 30.12 mmol) at 0 °C. The solution was stirred at room temperature for 24 hours, then neutralized by sodium hydroxide and extracted with ethyl acetate and sodium bicarbonate solution. The combined organic fractions were dried over anhydrous sodium sulfate, then the solvent was removed by rotary evaporation and dried further in vacuo. The residue was purified by column chromatography (5:1 hexane:CH_2Cl_2) to obtain **8** as a pure yellow solid (850 mg, 20%). ^{1}H NMR (500 MHz, $CDCl_3$, 25 °C): δ 6.02 (s, 4H), 4.41 (s, 4H). ^{13}C NMR (100 MHz, $CDCl_3$, 25 °C): δ 139.88, 105.31, 102.52, 20.58. LC-MS (ESI-TOF) m/z: $[M]^+$ Calcd for $C_{10}H_8Br_2O_4^+$ 349.8789; Found 349.8784.

Synthesis of Bisamine 9

Compound **8** (200 mg, 0.57 mmol) and hexamethylenetetramine (240 mg, 1.71 mmol) were dissolved in chloroform (10 mL) and refluxed for 24 hours. The yellow precipitate was collected by filtration and washed with cold chloroform. The solid was then dispersed into 15 mL ethanol and 2 mL concentrated hydrochloric acid and refluxed for an additional 24 hours. The flask was cooled to 0 °C and the solid was collected by filtration, washed with cold ethanol, and allowed to dry in open air. The solid was dispersed into 10% sodium carbonate solution (20 mL) and stirred, to which chloroform (20 mL) was then added. The biphasic solution was separated and the aqueous layer was further extracted with chloroform (3 × 20 mL). The combined organic phases were dried over anhydrous sodium sulfate and the solvent removed to yield **9** as a pale yellow solid (102 mg, 80%). ^{1}H NMR (500 MHz, CD_3CN, 25 °C): δ 5.87 (s, 4H), 3.68 (s, 4H). ^{13}C NMR (100 MHz, DMSO-d_6, 25 °C): δ 138.70, 108.47, 100.83, 35.56. LRMS (ESI-TOF) m/z: $[M+H-NH_2]^+$ Calcd for $C_{10}H_{11}NO_4^+$ 209; Found 209.

Synthesis of Macrocycle M5

To a solution of bis-amine **9** (100 mg, 0.45 mmol) and triethylamine (500 μL) in dry chloroform (500 mL) was added acid chloride **5** (115 mg, 0.45 mmol) in dry chloroform (50 mL) by syringe pump over 24 hours. After complete addition, the mixture was stirred for an additional 24 hours, after which the solvent was removed and the residue purified by column chromatography (1:3 $CHCl_3$:ethyl acetate) to yield **M5** as a white solid (38 mg, 21%). ^{1}H NMR (400 MHz, $CDCl_3$, 25 °C): δ 8.05 (s, 4H), 7.67 (s, 2H), 6.58 (t, J = 5.1 Hz, 4H), 5.85 (s, 8 H), 4.59 (d, J = 5.4 Hz, 8H), 1.36 (s, 18H). ^{13}C NMR: Limited solubility prevented ^{13}C NMR analysis. HRMS (ESI-TOF) m/z: $[M+Na]^+$ Calcd for $C_{44}H_{44}N_4NaO_{12}^+$ 843.2848; Found 843.2853.

Crystal Structure of Macrocycle M4b

An arbitrary sphere of data was collected on a colorless tablet-like crystal grown from a THF/hexanes solution. The specimen had approximate dimensions of 0.218 × 0.183 × 0.080 mm. Diffraction data were recorded on a Bruker APEX-II diffractometer using a combination of ω- and φ-scans of 0.5°.[30] Data were corrected for absorption and polarization effects and analyzed for space group determination.[31] The structure was solved

by dual-space methods and expanded routinely.[32] The model was refined by full-matrix least-squares analysis of F^2 against all reflections.[33] All non-hydrogen atoms were refined with anisotropic atomic displacement parameters. The asymmetric unit consists of one molecule of the macrocycle M4b and several diffuse, disordered solvent molecules. The solvent molecules appeared to be THF, but in the final analysis, solvent contribution was accounted for using the SQUEEZE routine in PLATON.[34] Two voids, each of 891 $Å^3$, were located. Electron density totaling 239 e^- in each void was accounted for. Crystal data for $C_{46}H_{48}N_4O_{14}$: M_r = 880.88; Monoclinic; space group $P2_1/n$; a = 16.2510(17) Å; b = 20.991(2) Å; c = 16.6756(17) Å; α = 90°; β = 96.331(2)°; γ = 90°; V = 5653.8(10) $Å^3$; Z = 4; T = 120(2) K; λ(Mo-Kα) = 0.71073 Å; μ(Mo-Kα) = 0.077 mm^{-1}; d_{calc} = 1.035 $g.cm^{-3}$; 76278 reflections collected; 11743 unique (R_{int} = 0.0624); giving R_1 = 0.0471, wR_2 = 0.1061 for 7850 data with [I>2σ(I)] and R_1 = 0.0812, wR_2 = 0.1189 for all 11743 data. Residual electron density ($e^-.Å^{-3}$) max/min: 0.256/−0.261. Atomic coordinates, bond lengths and angles, and displacement parameters have been deposited at the Cambridge Crystallographic Data Centre (CCDC number 1872795).

Association Measurements

A solution of 3.0 μM squaraine **S1** in chloroform was placed in a 1 mL quartz cuvette and titrated with aliquots from a macrocycle stock solution (300 μM macrocycle and 3.0 μM squaraine dye in chloroform). Following each addition of macrocycle, a fluorescence spectrum was acquired, and the squaraine emission at a single point was plotted to produce an isotherm that was fitted to a 1:1 binding model using Origin 8.1 software.

Kinetic Measurements

An aliquot of macrocycle solution (1.5 molar equivalents) in chloroform was added to a solution of 3.0 μM squaraine **S1** in chloroform and the increase in fluorescence intensity at a single wavelength (due to formation of the threaded complex) was monitored over time. The kinetic curve was fitted to second-order kinetic model using Origin 8.1 software.

Supplementary Material

Refer to Web version on PubMed Central for supplementary material.

Acknowledgements

This work was supported by the University of Notre Dame and a grant from the National Institutes of Health (GMR01059078).

Notes and references

1. Schalley CA, Weilandt T, Bruggemann J, and Vögtle F Top. Curr. Chem, 2004, 248, 141–200.
2. Hunter CA Chem. Commun, 1991, 749–751.
3. Eckelmann J, Saggiomo V, Sönnichsen FD, and Lüning U New J. Chem, 2010, 34, 1247–1250.
4. Howe ENW, Bhadbhade M, and Thordarson P J. Am. Chem. Soc, 2014, 136, 7505–7516. [PubMed: 24824365]
5. Xue M, Yang Y, Xiaodong C, Xuzhou Y, and Huang F Chem. Rev, 2015, 115, 7398–7501. [PubMed: 25734835]

6. Johnston AG, Leigh DA, Pritchard RJ, and Deegan MD Angew. Chemie Int. Ed, 1995, 34, 1209–1212.
7. Chang SY, Kim HS, Chang KJ, and Jeong KS Org. Lett, 2004, 6, 181–184. [PubMed: 14723523]
8. Destecroix H, Renney CM, Mooibroek TJ, Carter TS, Stewart PFN, Crump MP, and Davis AP Angew. Chem. Int. Ed, 2015, 54, 2057–2061.
9. Gassensmith JJ, Baumes JM, and Smith BD Chem. Commun, 2009, 6329–6338.
10. Gassensmith JJ, Barr L, Baumes JM, Paek A, Nguyen A, and Smith BD Org. Lett, 2008, 10, 3343–3346. [PubMed: 18582079]
11. Peck EM, Liu W, Spence GT, Shaw SK, Davis AP, Destecroix H, and Smith BD J. Am. Chem. Soc, 2015, 137, 8668–8671. [PubMed: 26106948]
12. Liu W, Peck EM, Hendzel KD, and Smith BD Org. Lett, 2015, 17, 5268–5271. [PubMed: 26452041]
13. Peck EM, Battles PM, Rice DR, Roland FM, Norquest KA, and Smith BD Bioconjug. Chem, 2016, 27, 1400–1410. [PubMed: 27088305]
14. Liu W, Gómez-Durán CFA, and Smith BD J. Am. Chem. Soc, 2017, 139, 6390–6395. [PubMed: 28426220]
15. Jacquemin D, Perpete EA, Laurent AD, Assfeld X, and Adamo C Phys. Chem. Chem. Phys, 2009, 11, 1258–1262. [PubMed: 19209370]
16. Liu W, Oliver AG, and Smith BD J. Am. Chem. Soc, 2018, 140, 6810–6813. [PubMed: 29787255]
17. Gassensmith JJ, Arunkumar E, Barr L, Baumes JM, DiVittorio KM, Johnson JR, Noll BC, and Smith BD J. Am. Chem. Soc, 2007, 129, 15054–15059. [PubMed: 17994746]
18. Fischer C, Nieger M, Mogck O, Böhmer V, Ungaro R, and Vögtle F Eur. J. Org. Chem, 1998, 155–161.
19. Weider PR, Hegedus LS, and Asada HJ. Org. Chem, 1985, 50, 4276–4281.
20. Pirnat K, Gaberscek M, and Dominko RJ. Power Sources, 2013, 235, 214–219.
21. Syper L, Meochowski J, and Kloc K Tetrahedron, 1982, 39, 781–792.
22. Murgu I, Baumes JM, Eberhard J, Gassensmith JJ, Arunkumar E, and Smith BD J. Org. Chem, 2010, 76, 688–691. [PubMed: 21166440]
23. Ke C, Destecroix H, Crump MP, and Davis AP Nat. Chem, 2012, 4, 718–723. [PubMed: 22914192]
24. Stewart P, Renney CM, Mooibroek TJ, Ferheen S, and Davis AP Chem. Commun, 2018, 54, 8649–8652.
25. Arunkumar E, and Ajayaghosh A Chem. Commun, 2005, 599–601.
26. Chen H, Farahat MS, Law K-Y, and Whitten DG J. Am. Chem. Soc, 1996, 118, 2584–2594.
27. Gassensmith JJ, Matthys S, Lee JJ, Wojcik A, Kamat PV, and Smith BD Chem. Eur. J, 2010, 16, 2916–2921. [PubMed: 20082394]
28. Al-Sayah MH, McDonald R, and Branda NR Eur. J. Org. Chem, 2004, 173–182.
29. Shaw S, Liu W, Gómez-Durán CFA, Schreiber C, de Lourdes Betancourt Mendiola M, Zhai C, Roland F, Padanilam S, and Smith BD Chem. Eur. J, 2018, 24, 13821–13829. [PubMed: 30022552]
30. APEX3 Bruker AXS, 2016 Madison, Wisconsin, USA.
31. Krause L, Herbst-Irmer R, Sheldrick GM, and Stalke DJ Appl. Crystallogr, 2015, 48, 3–10.
32. Sheldrick GM Acta Crystallogr, 2015, A71, 3–8.
33. Sheldrick GM Acta Crystallogr, 2015, C71, 3–8.
34. Spek AL Acta Crystallogr, 2009, D65, 148–155.

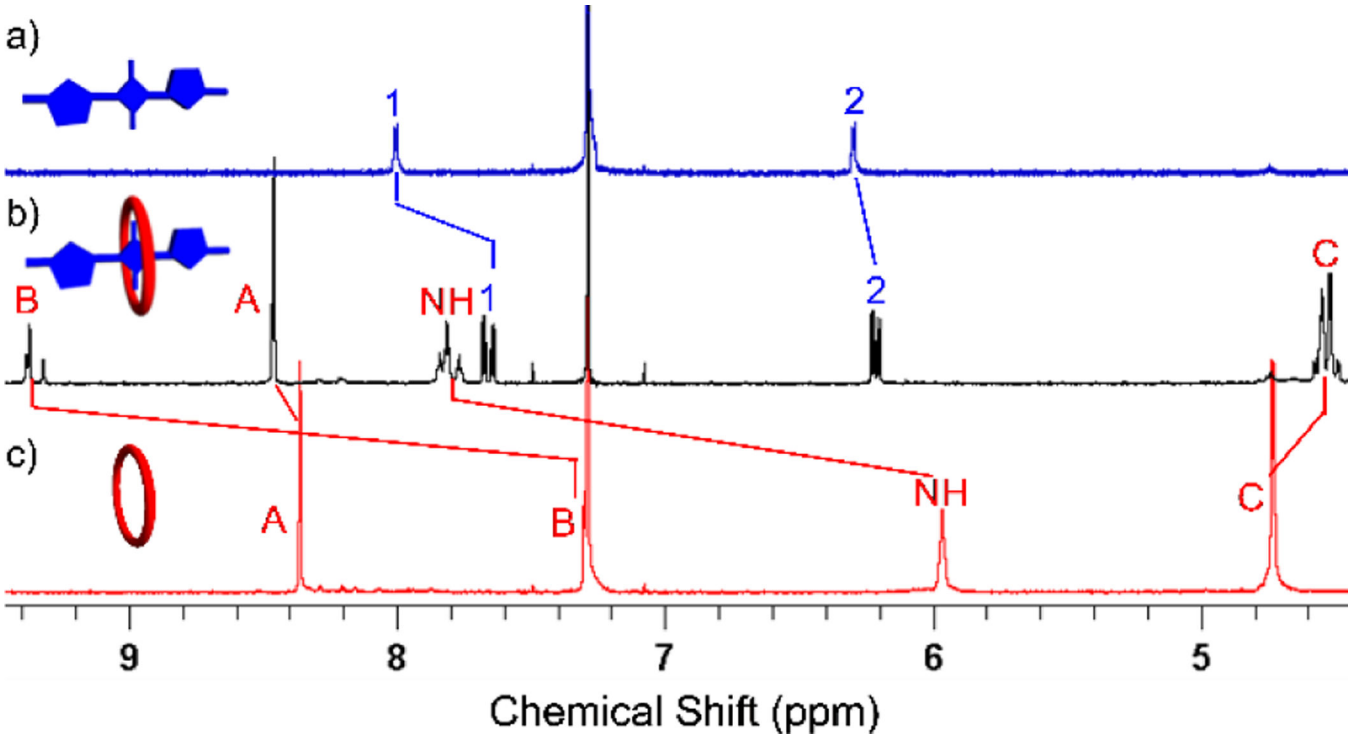

Fig. 1.

Partial ^{1}H NMR (500 MHz, $CDCl_3$) of a) **S1** (2.0 mM), b) **M3⊃S1** (2.0 mM), and c) **M3** (2.0 mM). Atom labels are provided in Scheme 1. The cartoons show **S1** (colored blue) with the two thiophene units in a trans orientation.

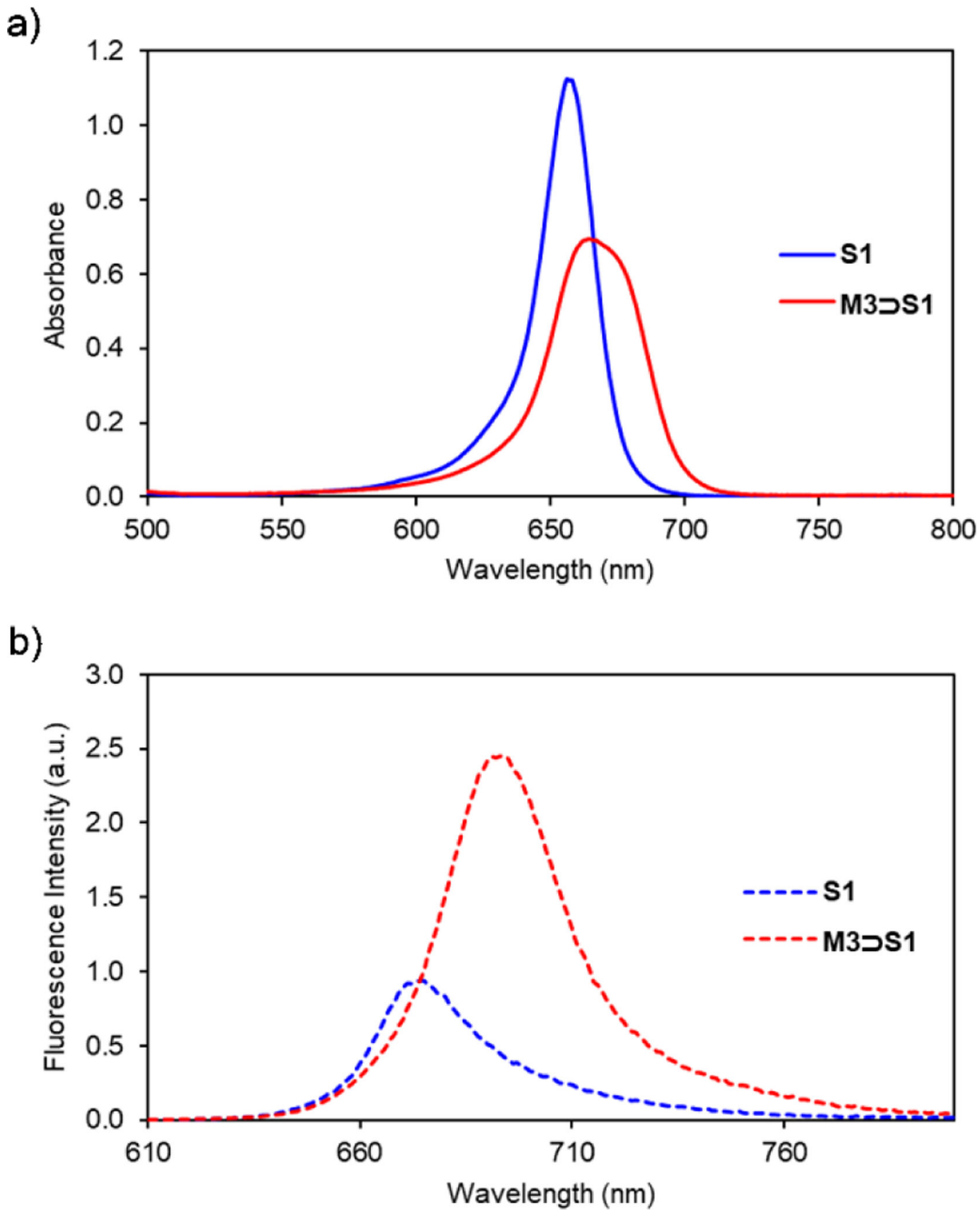

Fig. 2.

a) Absorption and b) emission maxima for solutions of **S1** or **M3⊃S1** in $CHCl_3$ (3.0 μM, ex. 600 nm, slit width: 2 nm at 25 °C).

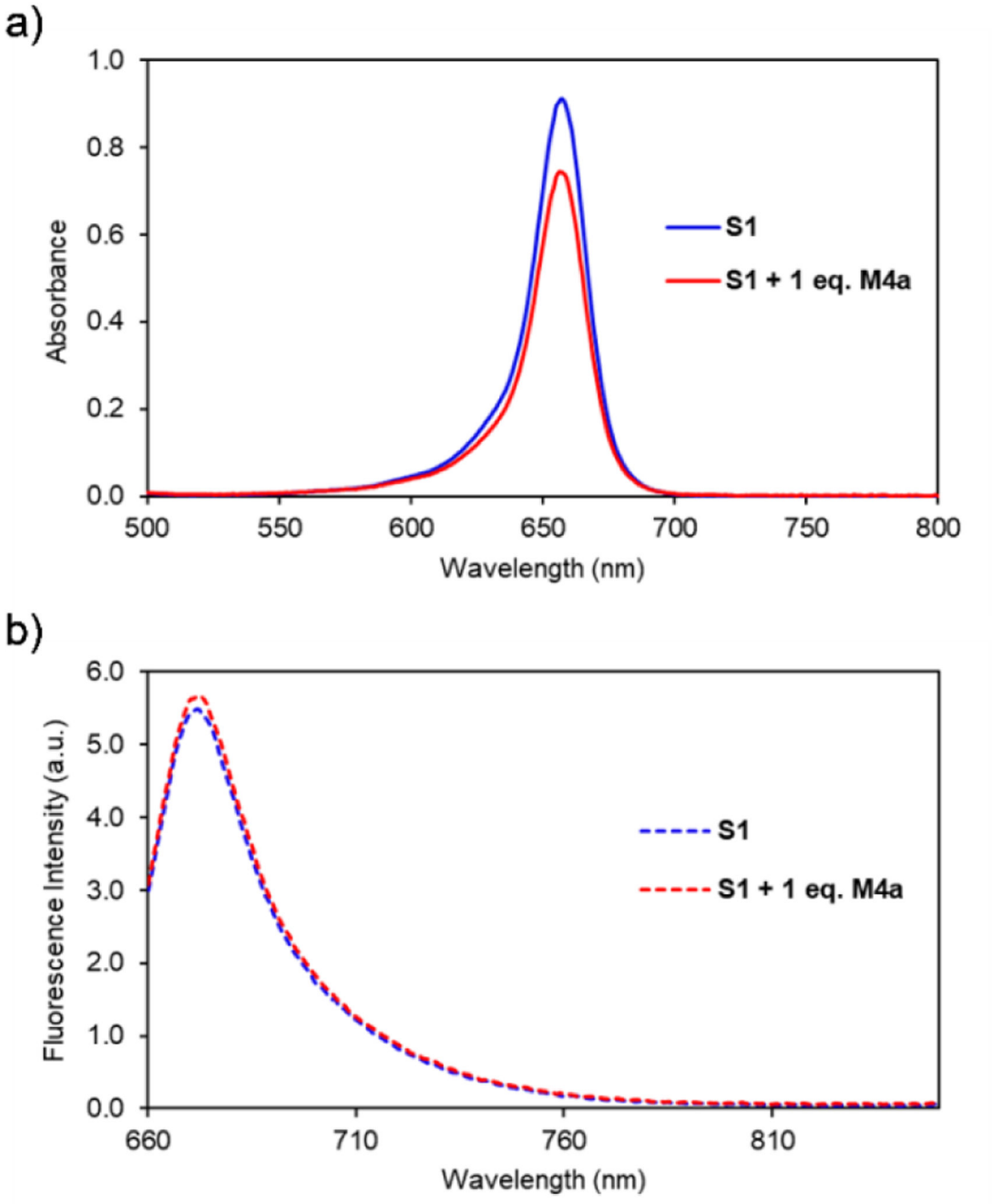

Fig. 3.

a) Absorption and b) fluorescence spectra of **S1** or **S1** with one equivalent of **M4a** in $CHCl_3$ (3.0 μM, ex. 650 nm, slit width: 2 nm at 25 °C).

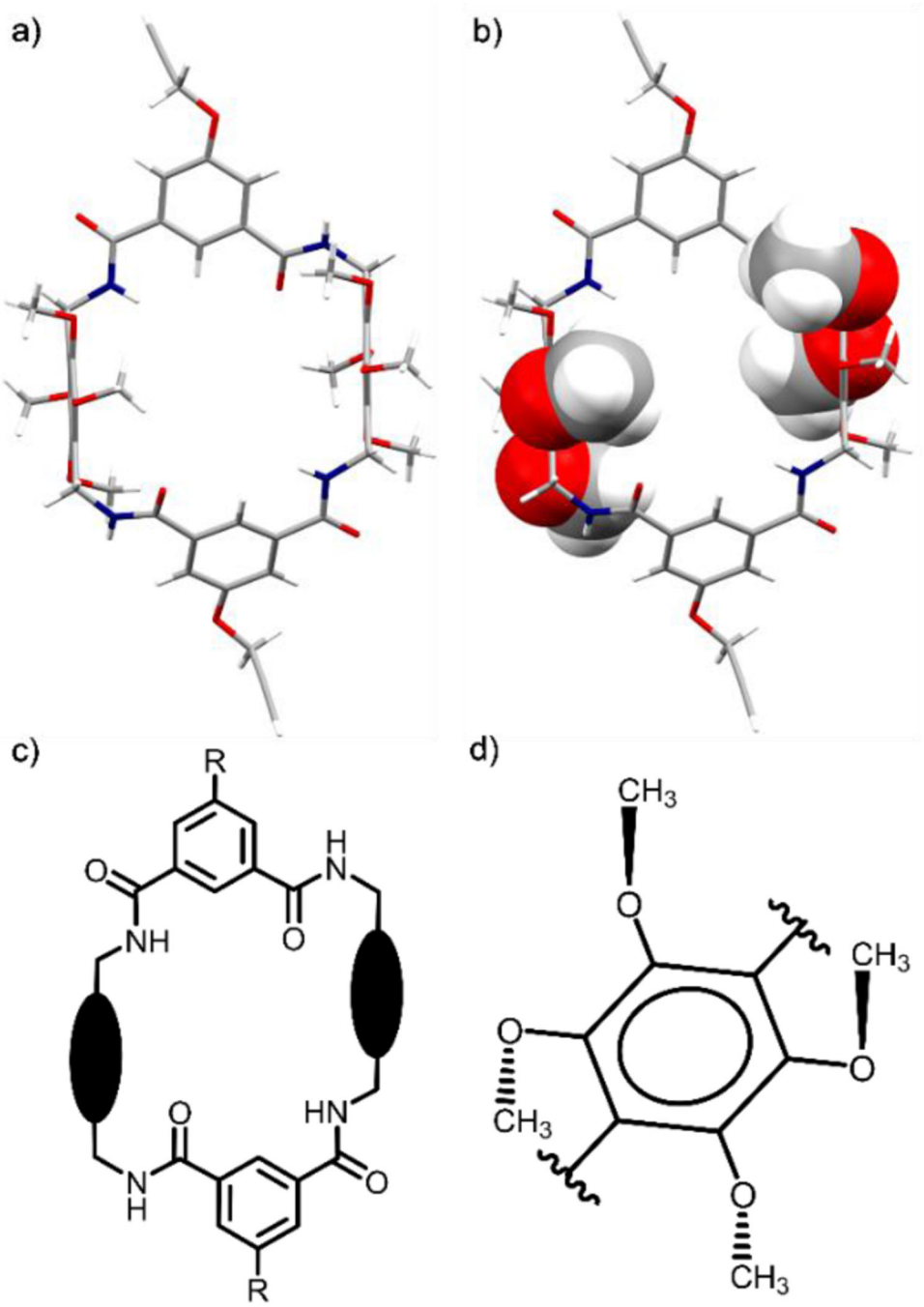

Fig. 4.

X-ray crystal structure of **M4b** illustrated as a) capped-sticks model and b) mixed model that emphasizes how the methoxy groups block front and rear access to the macrocyclic cavity. c) Schematic representation of the macrocyclic conformation of **M4b** with two of the four amide NH residues directed out of the cavity. d) Schematic representation illustrating how each pair of adjacent methoxy groups adopt a trans orientation relative to the plane of a phenyl sidewall in **M4b**.

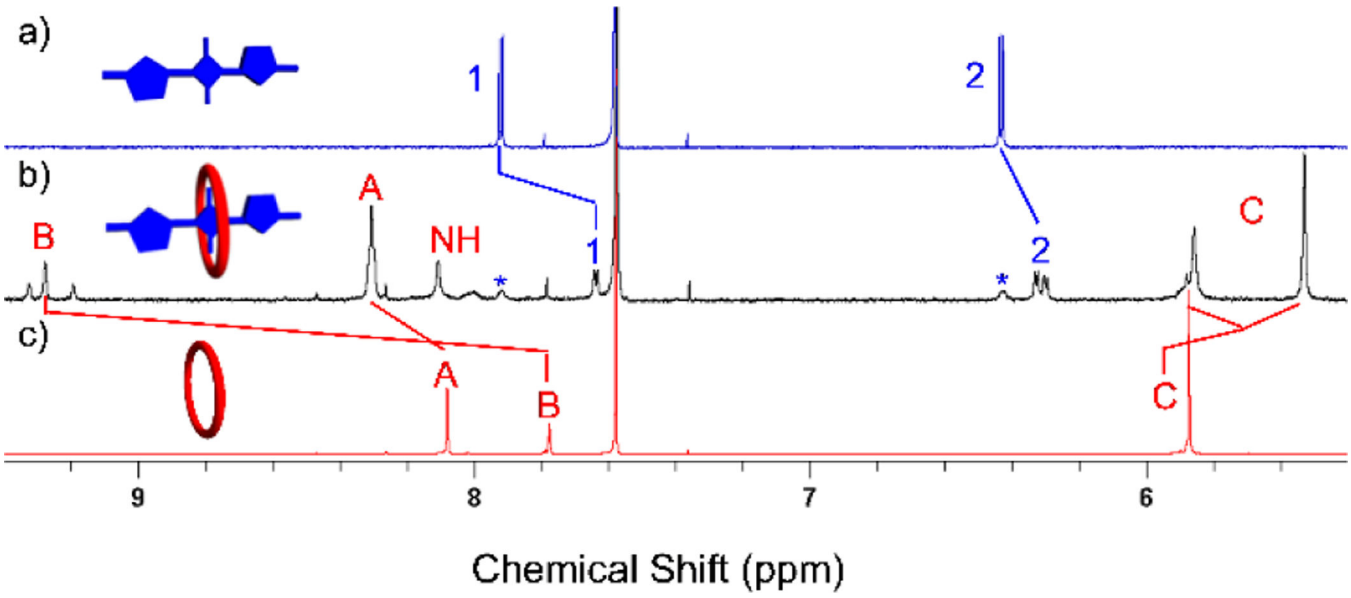

Fig. 5.

Partial ^{1}H NMR (500 MHz, 1:1 $CDCl_3$:CD_3OD) of a) **S1** (1.0 mM), b) **M5⊃S1** (1.0 mM, asterisks indicate signals for free **S1**), and c) **M5** (1.0 mM). Atom labels are provided in Scheme 1. The cartoons show **S1** (colored blue) with its two thiophene units in a trans orientation.

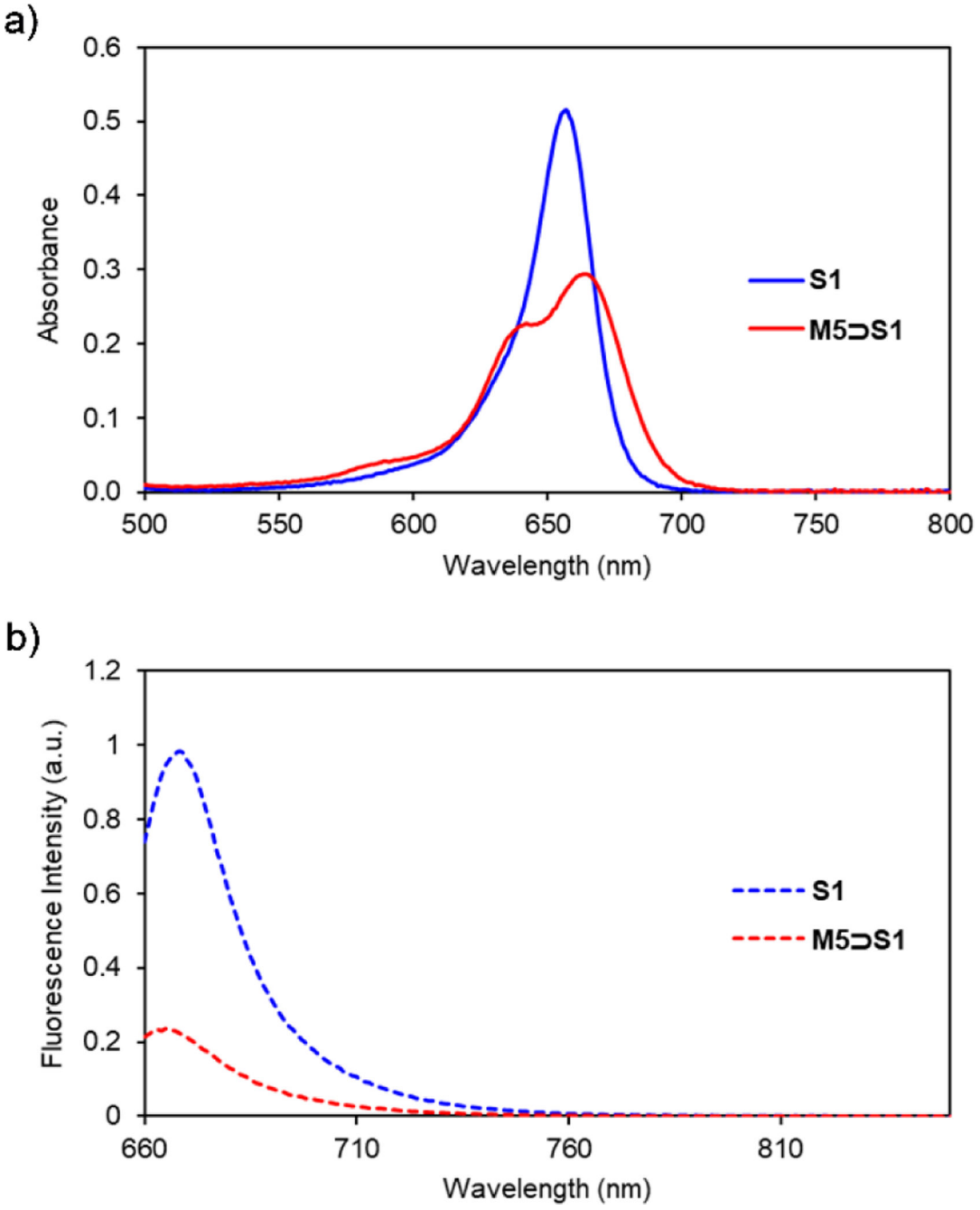

Fig. 6.

Changes in a) absorption and b) emission of **S1** and **M5⊃S1** in $CHCl_3$ (3.0 μM, ex. 650 nm, slit width: 2 nm at 25 °C).

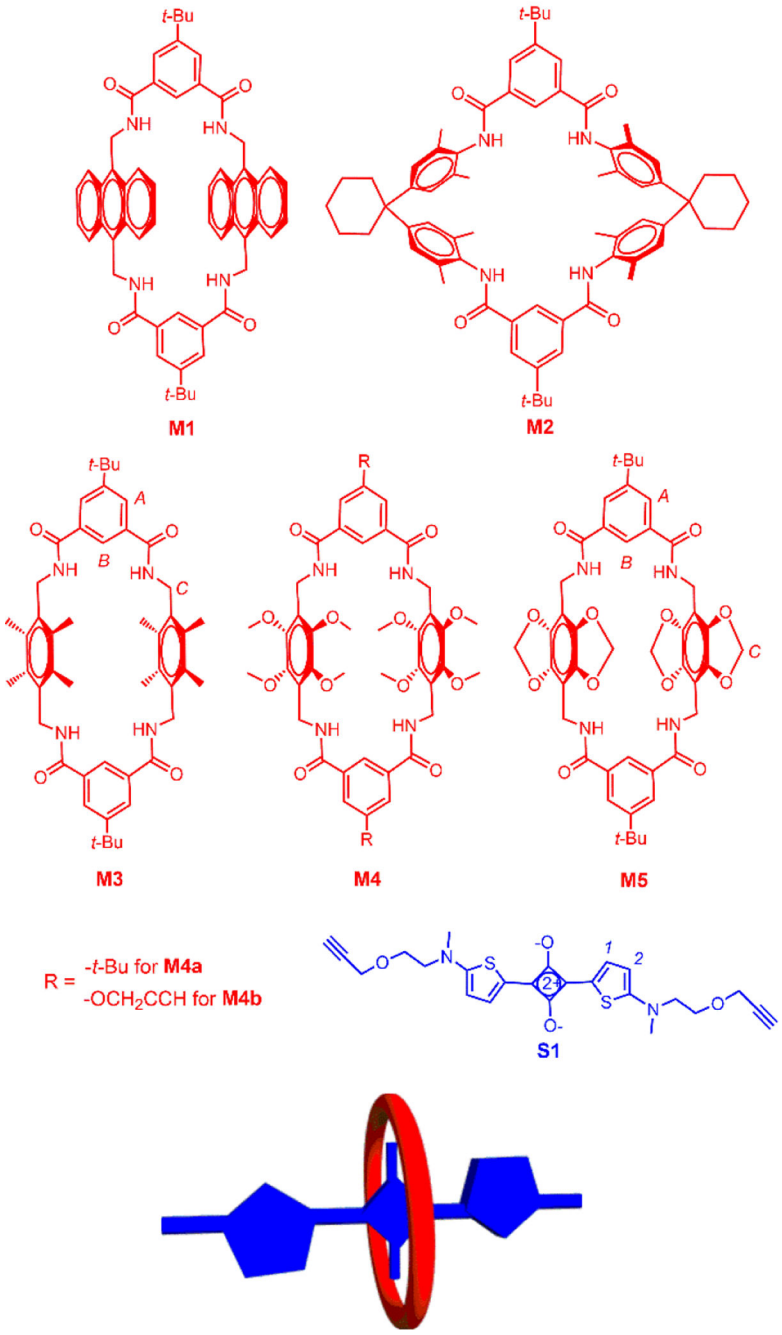

Scheme 1.

Structures of tetralactam macrocycles **M1-M5** and squaraine **S1** with relevant atom labels. Also shown is a cartoon of a threaded macrocycle/squaraine complex.

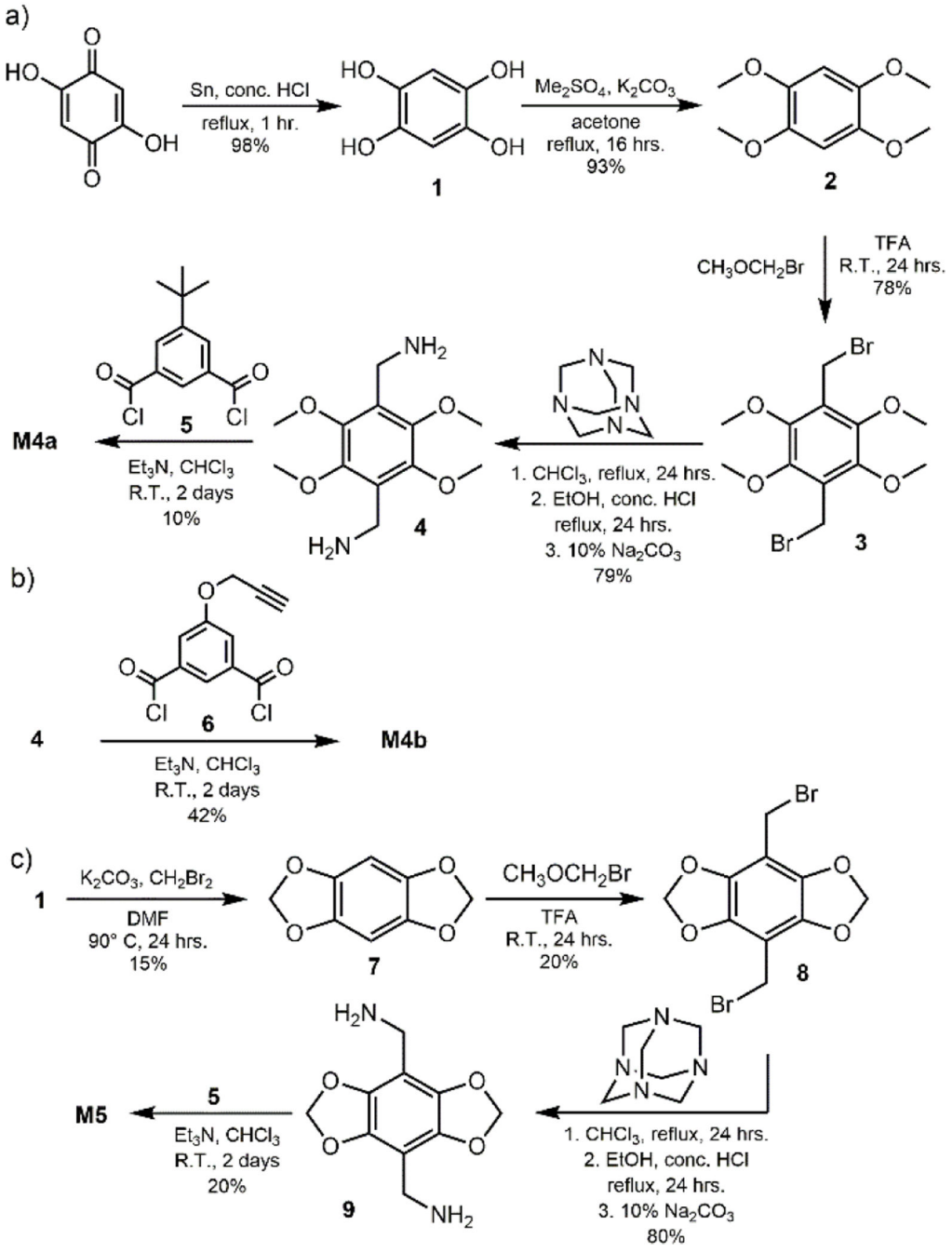

Scheme 2.
Syntheses of a) **M4a**, b) **M4b**, and c) **M5**.

Table 1

Photophysical data in $CHCl_3$ (3.0 μM) at 22 °C.

Compound	λ_{abs} (nm)	λ_{em} (nm)	log ε	Φ_f [a]
S1	656	675	5.575	0.09
M3⊃S1	664	694	5.365	0.45

[a] relative to bis[4-(N,N-dimethylamino)phenyl]squaraine (Φ_f = 0.70 in chloroform).

Table 2

Association constant (K_a) and rate constant (k_{on}) for complex formation in $CHCl_3$ (3.0 μM) at 22 °C.

Complex	K_a (M^{-1})	k_{on} ($M^{-1}s^{-1}$)
M3⊃S1	$(5.1 \pm 2.9) \times 10^6$	$(9.1 \pm 1.1) \times 10^3$
M1⊃S1[a]	$(7.7 \pm 0.8) \times 10^7$	$(8.0 \pm 0.3) \times 10^4$

[a] Data taken from reference 12.